Orthorhombic low-temperature superstructures in $YBa_2Cu_3O_{6+x}$

P. Manca* and S. Sanna

Istituto Nazionale per la Fisica della Materia (INFM) and Dipartimento di Fisica, Università di Cagliari, 09042, Monserrato (CA), Italy

G. Calestani

Dipartimento di Chimica G.I.A.F., Università di Parma, Viale delle Scienze 7a, 43100 Parma, Italy

A. Migliori

CNR-LAMEL Area della Ricerca di Bologna, Via Gobetti 101, 40129 Bologna, Italy

S. Lapinskas

Faculty of Physics, Vilnius University, Saulėtekio 9, 2054 Vilnius, Lithuania

E. E. Tornau

Semiconductor Physics Institute, Goštauto 11, 2600 Vilnius, Lithuania

The emergence of the cell-doubled (OII) and both cell-tripled (OIII and OIII*) phases of $YBa_2Cu_3O_{6+x}$ are observed on oxygen-chain-equalized and order-stabilized pair samples at an extended range of oxygen concentrations ($0.28 < x < 0.83$), including the interval of x, which is characteristic of the onset of superconductivity. The phase diagram for the asymmetric next-nearest-neighbor interaction model, extended to include an additional longer-range interaction potential between oxygen atoms, is calculated and compared to two experimental phase diagrams, obtained for intercalated as well as for deintercalated members of the pair samples. A fairly good agreement with experimental data on locations of the OII, OIII, and OIII* phases in the phase diagram and on the average length of the O-Cu-O chains is obtained.

PACS number(s): 74.72.Bk, 64.60.Cn, 61.14.−x

I. INTRODUCTION

The studies of oxygen ordering in high-T_c superconductor $YBa_2Cu_3O_{6+x}$ were very popular in the 1990's, since the superconducting temperature of this compound was found to be related to different types of oxygen order in the basal plane. The recent revival of interest in this phenomenon and, subsequently, in the asymmetric next-nearest-neighbor interaction (ASYNNNI) model, which was used to describe it, is caused by achievements in sample preparation and studies[1–3] of oxygen superstructures occurring in the basal plane of this compound.

During the last decade the occurrence of orthorhombic superstructures of $YBa_2Cu_3O_{6+x}$ was observed by electron,[4–7] x-ray,[2,3,8–11] and neutron[2,9] diffraction, and electron microscopy.[12] The cell-doubled OII phase was observed at the interval of oxygen concentration around its stoichiometry $x = 0.5$ (Refs. 3–5,8,10, and 12) and even at values of an oxygen amount as low as $x = 0.32$.[7] The cell-tripled OIII phase with oxygen stoichiometry at $x = 0.67$ was found at $x = 0.65$ (Ref. 13) 0.7, 0.73 (Ref. 11), 0.77 (Ref. 9), 0.72, 0.83, (Ref. 2) and 0.67–0.75.[6] These phases are characterized by short-range order, quasi-two-dimensionality, and "full-empty" (OII) and "full-full-empty" (OIII) sequences of the O-Cu-O chains along the a axis in the basal plane of $YBa_2Cu_3O_{6+x}$. The main orthorhombic structure OI with oxygen stoichiometry at $x = 1$ is characterized by the "full-full" sequences of the O-Cu-O chains and long-range order resulting in sharp Bragg peaks.

The calculations of oxygen ordering for $YBa_2Cu_3O_{6+x}$ are usually based on the ASYNNNI model[14] with nearest-neighbor (NN) ($v_1 > 0$) and next-nearest-neighbor (NNN) ($v_2 < 0$ and $v_3 > 0$) oxygen atom interactions taken into account. The OIII phase is demonstrated[15] to occur in the (T,x) phase diagram of $YBa_2Cu_3O_{6+x}$ if the repulsive interaction $v_4 > 0$ of next-nearest O-Cu-O chains (NNC) is also considered. Each additional repulsive constant of interaction along the a axis v_3, v_4, etc. leads to a system of so-called branching phases at low temperatures.[16] Accounting for the v_4 interaction marks the second branching level, the occurrence of the OIII phase between the OI and the OII phases. The surprising result of the phase diagrams thus obtained[15,17] was the "intrusion" of the OI phase between the phase regions of the OII and OIII phases (i.e., at $0.5 < x < 0.6$), and the stability of the OI phase in this region down to the absolute zero temperature. This result has never been supported by experiments.[6,11] Therefore two extended models with an additional attractive longer-range interaction, that was assumed to be related to interplane coupling[18] or strain[19] and that had a magnitude on the order of v_4 were proposed. However, more elaborate calculations[17] have shown that the model truncated at v_4 is quite sufficient, and the superlattice reflections of both "neighboring" phases OII and OIII are clearly seen even in the region of "intrusion" of the OI phase $0.5 < x < 0.6$. Moreover, the intrusion might be partially blocked by the occurrence of an incommensurate phase in that region. Several alternative models for the calculation of low-temperature oxygen superstructures have been used in Refs.

20–22. These long-range models can potentially describe a variety of chain (OII, OIII, OV, etc.) and even nonchain [$\sqrt{2}x2\sqrt{2}$ or $2\sqrt{2}x2\sqrt{2}$ (Refs. 8 and 12)] superstructures. But since the experimental evidence on superstructures with periodicity exceeding $3a$ is still very vague (some indications might be found however in Refs. 2,5, and 12), here we use the short-range ASYNNNI model, extended to include the interaction v_4, which is the minimal model, quite sufficient to describe the experiments on pair samples.[6]

In spite of its extreme interest (since it comprises the onset of superconductivity around $x=0.3$), calculation on the oxygen-deficient side of the phase (x,T) diagram with the higher-order superstructures taken into account has never been performed before. There are two reasons for this. First, the opinion prevailing was that the calculation for $x>0.5$ was quite sufficient, since the regions of the OIII phase (''full-full-empty'' sequences of the O-Cu-O chains) and OIII* phase (''full-empty-empty'' sequences of the O-Cu-O chains) have to be symmetric on the phase diagram with respect to point $x=0.5$. However, this conclusion is not evident, since the phase diagram of the original ASYNNNI model is not symmetric with respect to this point due to prevalence of the tetragonal (T) phase at higher temperatures and $x<0.5$. The second (and main) reason is due to a very slow oxygen diffusion at low oxygen concentrations and therefore to the difficulty of having reliable orthorhombic samples with well-expressed O-Cu-O chains. This difficulty has recently been removed[6] using oxygen-equalized and order-stabilized $YBa_2Cu_3O_{6+x}$ pair samples, prepared under identical thermal conditions, one by intercalation [I] and the other by deintercalation [D] of oxygen atoms. This preparation method allowed us to investigate, in a comparative way, the low-temperature evolution of oxygen ordering in the basal plane of this compound. The study was at first performed on the domains of existence of the OII and OIII superstructures and then on the transient tetragonal-orthorhombic (T-O) region. This resulted in the experimental determination of the phase diagram for both [I] and [D] samples in an extended compositional range and stimulated us to calculate the phase diagram in order to compare the experimental and calculated phase diagrams. We also calculated the average lengths of O-Cu-O chains in tetragonal, OIII*, OII, OIII, and OI phases and compared them with those obtained by the nuclear quadrupole resonance (NQR) measurements[7] on the [I] and [D] pair samples.

II. PHASE DIAGRAM

A. Experiment

The study of oxygen ordering and related structural and superconducting transitions along the T-O line of the low-temperature ($75-130\,°C$) phase diagram was performed on bulk polycrystalline oxygen-equalized pair samples within the range $0.28<x<0.83$. The fabrication of these samples can be viewed as a topotacticlike process, where the stoichiometric end terms of $YBa_2Cu_3O_{6+x}$ [the fully oxygenated OI phase ($x\sim1$) and the reduced T phase ($x\sim0$) derived from it] are equalized under vacuum, one by deintercalation and
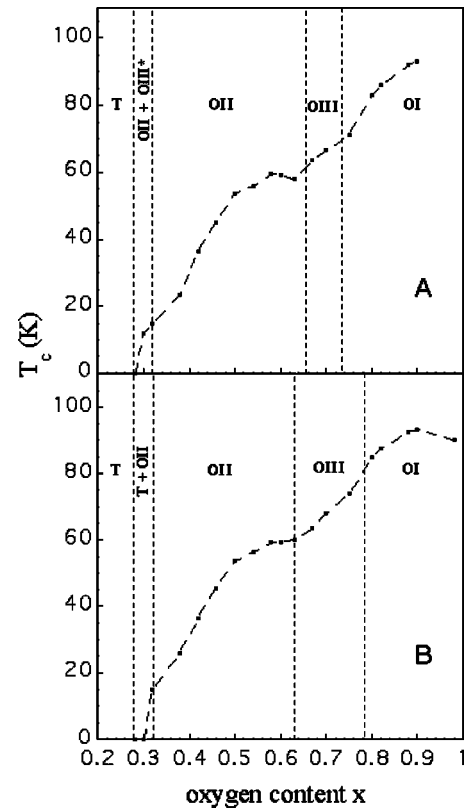

FIG. 1. Superconducting temperature as a function of oxygen amount for intercalated (a) and deintercalated (b) oxygen-chain-equalized pair samples. The superstructures are determined by electron diffraction.

the other by intercalation of intrinsic oxygen atoms into the basal CuO_x plane.[6] The samples were equalized at $T_e=450-670\,°C$ for a time ranging from one month to one day, respectively, and then slowly cooled ($1\,°C/min$) and order stabilized over three days at a composition-dependent stabilization temperature ($T_s=75\,°C$ for samples in the composition range $0.28\leq x\leq0.32$, $T_s=75\div130\,°C$ for $0.32<x\leq0.63$, and $T_s=75\,°C$ for $0.63<x\leq0.83$). The structural characterization was performed by electron diffraction (ED), since this technique (owing to the fact that the scattering amplitudes for electrons are 10^3 times the ones for x rays) is a very powerful tool for detecting structural order on the microscopic scale.

The structural phase diagrams resulting from intercalation and deintercalation were studied simultaneously by using [I] and [D] pair samples with the same oxygen content. For each sample the ED measurements were performed on a large number of crystalline grains to achieve sufficient statistics. As a result, with the increase of x both [I] and [D] phase diagrams can be divided into five regions: T, transient T-O, OII, OIII, and OI (see Fig. 1). However these regions differ in the compositional extension, revealing that even for well-equilibrated samples kinetic factors should be taken into account. The comparative studies[6] showed that the different kinetic nature of intercalation and deintercalation processes can lead (depending on the composition) to the same as well as different local oxygen ordering. Equivalence of the
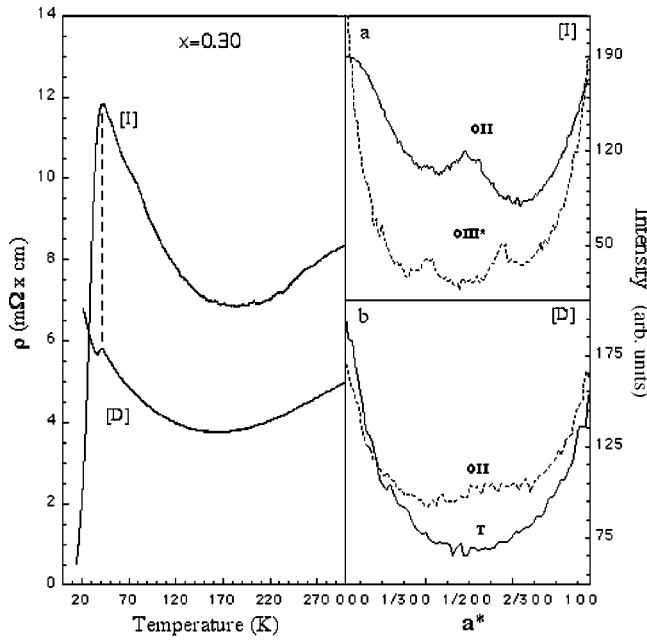
FIG. 2. Comparative resistive and structural behavior observed for $[I]_{0.30}$ and $[D]_{0.30}$ samples at the transient T-O region showing the coexistence of the (OII+OIII*) orthorhombic superstructures in the superconducting phase for the [I] sample (a) and the (T+OII) phases in the nonsuperconducting phase for the [D] sample (b).

FIG. 3. T_c splitting and related ED patterns for the $[I]_{0.63}$ and $[D]_{0.63}$ pair samples showing the microdensitometer trace ($\frac{1}{2}00$) of the OII [I] phase and the ($h/300$) of the OIII [D] phase at the phase boundary OII-OIII.

O-Cu-O chains' arrangement of the [I] and [D] samples of the same oxygen content results in an equal superconducting transition temperature (T_c singularity), as well as inequivalence in T_c splitting ($\Delta T_c \neq 0$). These peculiar kinetic aspects of oxygen ordering cannot be directly observed in experiments on single samples.

The T-O transient region ($0.28 \leq x \leq 0.32$) is a remarkably complex zone when studied comparatively using pair samples with the same oxygen content and thermal history. Similar structural and electronic characteristics of both [I] and [D] samples are observed only for the oxygen contents $x = 0.28$ and $x = 0.32$, which are the highest and the lowest composition limits for the existence of the T and the OII phases, respectively. The $[D]_{0.28}$ and $[I]_{0.28}$ samples show a temperature dependence of resistivity $\rho(T)$, typical of thermally activated electronic processes, while the $[D]_{0.32}$ and $[I]_{0.32}$ samples manifest superconducting properties. The T-O transient zone between $x = 0.28$ and 0.32 is a two-phase region in which related structural and electronic properties can be observed comparatively for homologous [D] and [I] samples, e.g., at $x = 0.30$.[7] In this region the O-Cu-O chain growth along the b axis at the transition from the T ($a = b$) to O ($a \neq b$) phase develops in a different way for the $[D]_{0.30}$ and $[I]_{0.30}$ samples and manifests itself as structural and electronic phase separation. In the initial stage the anisotropic chain growth develops with periodicity $2a$ or $3a$, preferentially for the $[I]_{0.30}$ samples. Diffuse satellite spots ($h/200$) or ($h/300$) associated with orthorhombic OII or OIII* superstructures, respectively,[1] characterize the [I] grains, whereas a phase segregation in a majority of T and a minority of OII domains is observed for the [D] samples. In Fig. 2 we comparatively show the typical $\rho(T)$ curves of the $[D]_{0.30}$ and
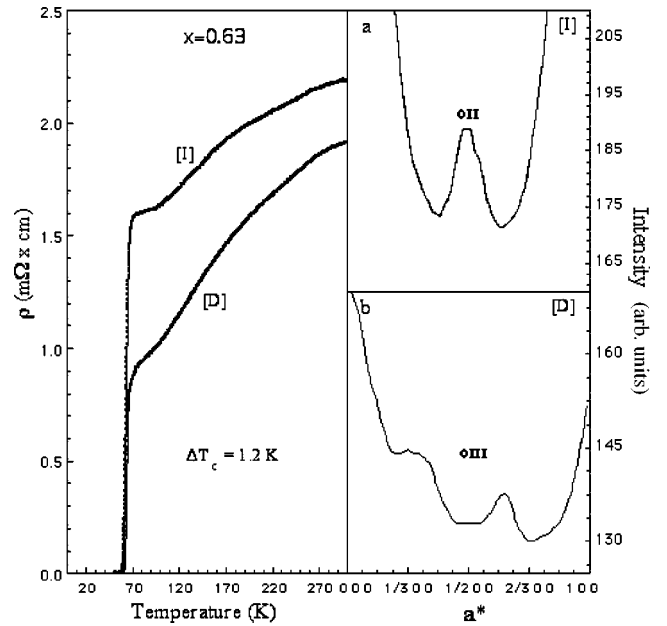
$[I]_{0.30}$ samples as well as related microdensitometer traces of the ED patterns. The resistive steplike discontinuity at ~ 40 K appears to be structurally related to the OIII*-phase ordering in the superconducting $[I]_{0.30}$ sample, whereas the coincidence of the resistive kink in (T+OII) $[D]_{0.30}$ and the T_c onset in (OII+OIII*) $[I]_{0.30}$ indicates that the short-range order in the minority of the OII component phase of [D] samples should be quite similar to that of the [I] samples. However, during the chain-to-plane charge transfer, the O-Cu-O chain fragments of the $[I]_{0.30}$ sample appear to be "more effective" than those of the $[D]_{0.30}$. This is due to different average chain lengths (l) as observed recently by the NQR spectra:[7] $l_I = 3.9$ for the superconducting $[I]_{0.30}$ samples as compared to $l_D = 1.9$ for the nonsuperconducting $[D]_{0.30}$ samples. This finding is in a perfect agreement with the theoretical prediction[20,23] that there is essentially no charge transfer from the chain fragments shorter than three oxygen atoms.

The OIII* ordering, observed preferentially in intercalated samples equilibrated at $450\,°C$, appears to be a metastable precursor of the OII ordering. After a long-term (one year) aging of the $[I]_{0.30}$ samples at room temperature the ($h/300$) superstructure reflections disappear and the original two-phase state (OII+OIII*) stabilizes into the OII phase.

Starting with $x = 0.32$ oxygen ordering develops within three structural domains, defined by the orthorhombic structures OII, OIII, and OI, which determine a typical evolution of the T_c dependence on oxygen content.[1] The OII phase is observed in both phase diagrams in the x range $0.32-0.63$ and the OIII phase in the range $0.65-0.73$. Again, as observed previously for the range $0.28-0.32$, the different kinetic nature leads to different behavior of the [D] and [I] pairs in the transition regions OII-OIII and OIII-OI, which is
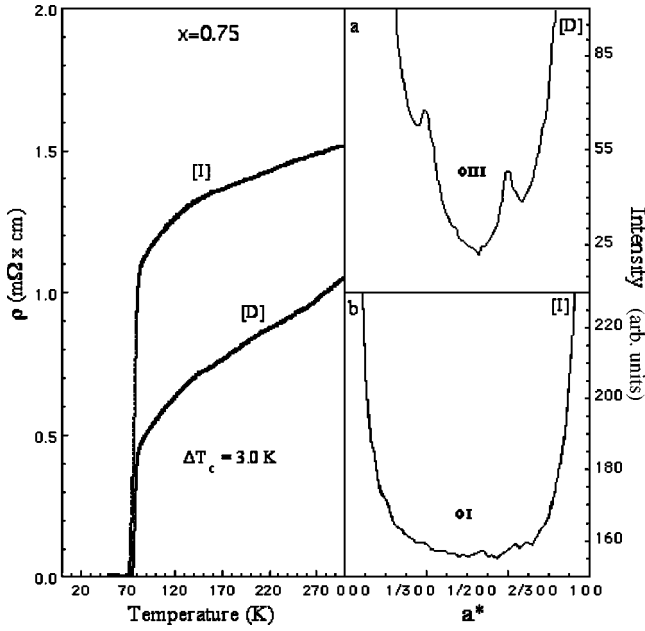
FIG. 4. T_c splitting and related ED patterns for the $[I]_{0.75}$ and $[D]_{0.75}$ pair samples showing the microdensitometer trace of the fundamental structure OI [I] and the ($h/300$) of the OIII [D] superstructure at the phase boundary OIII-OI.

manifested as T_c splitting and phase separation between ordered structures with the same oxygen content (see Figs. 3 and 4). In general, the differences observed in these transition regions reveal the tendency of the system to retain the OII structure when x is increased above or decreased below 0.5. The latter effect is demonstrated, e.g., in the occurrence of the phase transition OII→OIII at higher x than the corresponding reverse transition OIII→OII (see Fig. 1). Moreover the system seems to favor the triple-cell ordering when oxygen is deintercalated from fully occupied chains (OIII) or intercalated in vacant chains (OIII*) (the OIII region is more extended in [D] samples whereas the OIII* region is present only in [I] samples). We have found that the best OII ordering (alternate full-empty chains) is accomplished for oxygen content $x=0.57$. This clearly deviates from the ideal stoichiometric value $x=0.50$ and agrees with previously reported results.[5] Both $[D]_{0.57}$ and $[I]_{0.57}$ $\rho(T)$ curves show almost equivalent temperature evolution and T_c singularity related to very sharp ($h/200$) reflections.[6] In a similar way the full-full-empty sequence (OIII superstructure) appears to be best realized in the $x=0.70$ pair, which is characterized by sharp ($h/300$) spots, more elongated in the $[I]_{0.70}$ sample than in the corresponding $[D]_{0.70}$ sample.

B. Cluster-variation-method calculation

In this work we calculate the phase diagram of $YBa_2Cu_3O_{6+x}$ using the extended ASYNNNI model. For the first time the phase diagram is widened to $x<0.5$ to include the experimentally observed OIII* phase. The two-dimensional lattice-gas Hamiltonian of our model has the form

$$\mathcal{H} = v_1 \sum_{NN} n_i n_j + v_2 \sum_{\substack{NNN \\ (\text{over Cu})}} n_i n_j + v_3 \sum_{NNN} n_i n_j$$

$$+ v_4 \sum_{NNC} n_i n_j - \mu \sum_i n_i . \tag{1}$$

The occupancy numbers are $n_i=1$ (0), if the site i of the basal plane lattice is occupied (unoccupied) by an oxygen atom, the summation runs over NN, NNN, NNN (over Cu) and NNC oxygen sites and μ stands for oxygen chemical potential.

There are two sublattices of oxygen atoms in the basal plane [so-called O(1) and O(5) oxygen atoms]. In the tetragonal phase concentrations of both sublattices, $c_{O(1)} = c_{O(5)}$, where $c_k = \langle n_i^k \rangle$, but in the OI phase $c_{O(1)} > c_{O(5)}$. The ground state of the OI phase at $x = c_{O(1)} + c_{O(5)} = 1$ corresponds to fully occupied O(1) and a vacant O(5) sublattice. The occurrence of the OII phase is caused by the cell doubling: the sublattice O(1) splits into two symmetric sublattices with an equal number of sites, and the ground state of this phase at $x=0.5$ corresponds to fully occupied $O(1)_1$ and vacant $O(1)_2$ and O(5) sublattices. The order parameter of this phase is $c_{O(1)_1} - c_{O(1)_2}$. In the OIII and OIII* phases we can define two unequivalent O(1) and two unequivalent O(5) sublattices, with the number of sites in the $O(1)_1$ sublattice being twice that in the $O(1)_2$. The ground states then correspond to fully occupied $O(1)_1$, vacant $O(1)_2$, and both O(5) sublattices for $x=0.67$, and fully occupied $O(1)_2$, vacant $O(1)_1$, and both O(5) sublattices for $x=0.33$. Our calculation is performed by the $13+12$-point approximation of the cluster-variation method (CVM). The 13-sites basic cluster, the largest used so far, comprises nine (3×3) sites of sublattice O(1) and four sites of sublattice O(5) located inside this 3×3 cluster (and vice versa). The 12-sites cluster is formed by six sites of both O(1) and O(5). The basal plane of $YBa_2Cu_3O_{6+x}$, with indication of oxygen sublattices and constants of interaction, can be found, for example, in Ref. 17. From the first-principles electronic structure calculations two sets of the main interaction constants of the ASYNNNI model were obtained: $v_1=6.9$ mRy, $v_2/v_1=-0.35$, $v_3/v_1 = 0.16$ (Ref. 24), and $v_1=6.71$ mRy, $v_2/v_1=-0.83$, $v_3/v_1=0.11$.[25] The value of the longer-range repulsive interaction v_4 can be determined by comparing experimental and theoretical curves. For example, $v_4=0.037v_1$ was obtained[17] from a fit of the temperature dependence of the diffuse peak intensity of the corresponding x-ray-diffraction data for the OIII-phase ($x=0.77$) sample.[9] It should be noted that we have excluded from the Hamiltonian (1) two next-nearest-neighbor interactions that are shorter range than the v_4 interaction. These interactions are irrelevant for the formation of the OIII phase and cannot change the phase diagram essentially.[15] As can be seen (Fig. 5), the phase diagram, obtained using the first set of interaction constants and $v_4=0.037v_1$, is more or less symmetric with respect to point $x=0.5$ at low temperatures ($T<350$ K), but at higher temperatures the influence of the tetragonal phase and mixed tetragonal and orthorhombic phases is observed. At both sides of the OII phase the orthorhombic OIII* and OIII
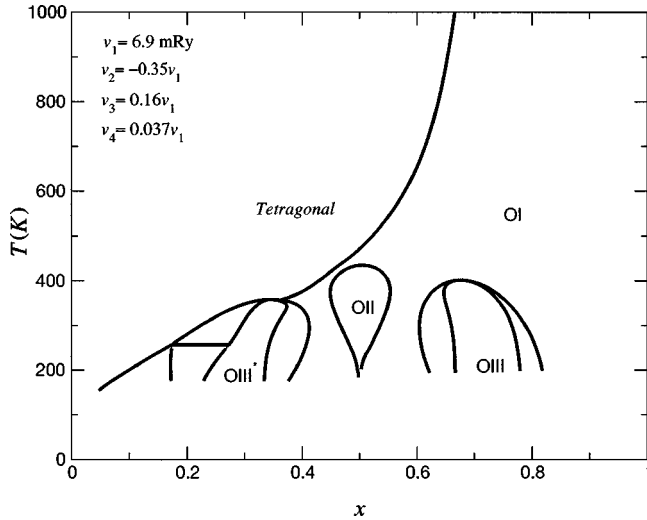
FIG. 5. Phase diagram, obtained by the $13+12$-point CVM with the interaction constants $v_1 = 6.9$ mRy, $v_2/v_1 = -0.35$, $v_3/v_1 = 0.16$, and $v_4/v_1 = 0.037$.
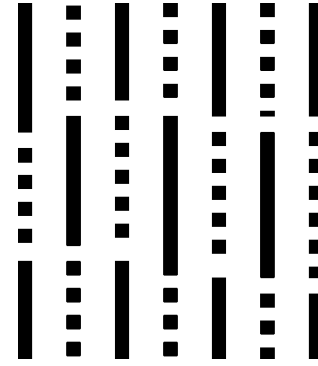
FIG. 6. Fragment of thermodynamic OI phase at $x > 0.5$, obtained by model (1), giving the diffraction pattern of the OII phase. The O(5)-oxygen sublattice, empty at low temperatures, is not shown. Occupied O(1)-Cu-O(1) chains are shown by solid, empty v-Cu-v chains by dotted lines.

phases are seen. The areas of these phases on the phase diagram are comparable to the area occupied by the OII phase.

Here we would like to discuss the phase boundaries of the ordered phases by comparing the phase diagrams obtained by the CVM (see Ref. 17 and this work) and the Monte Carlo method (see e.g., Ref. 2). Note, that in the latter calculations no narrowing of the OII phase at low temperatures is observed and therefore its area at low temperatures extends almost to the interval $0.3 < x < 0.6$.

The phase boundaries, obtained by the CVM, divide the thermodynamic phases obtained from minimization of the free energy exhibiting symmetry breaking at the second-order phase transition. For the original ASYNNNI model ($v_4 = 0$) the ground states of the OII phase in the phase diagram are indeed found in the interval $0.3 \lesssim x \lesssim 0.7$. Accounting for the v_4 Eq. (1) leads to the phase diagram in Fig. 5. The ground state of the OII phase is found only for $x = 0.5$; for all nonstoichiometric values of oxygen amounts close to $x = 0.5$, $c_{O(1)_1} = c_{O(1)_2}$ and, rigorously, the OI phase should be considered the real thermodynamic phase. The reason for this phenomenon is most likely related to the influence of entropy. What we find in our CVM calculations is that the OII phase exhibits long-range superstructure correlations due to cell doubling. Even in the neighboring OI phase (between the OII and OIII phases) there also exists[17] rather long-range correlations characteristic of the OII phase that result in considerable diffuse peaks in diffraction patterns, and the sizes of these correlations are comparable to typical system sizes used in Monte Carlo correlations [cf. 70 unit cells along the a axis for the best OII samples produced up to now[3] and 128×128 lattices (64 unit cells) taken for calculations]. Thus if we determine the phase from the structure factor (as in experiments or Monte Carlo calculations) we end up with a bell-shaped OII phase in the phase diagram with smeared phase boundaries. Using the CVM we obtain the narrowing of the OII phase at low temperatures and diffuse peaks of the OII phase in the neighboring insertions of the OI phase. The

best illustration is Fig. 6, which shows a typical situation of O-Cu-O chains for the model (1) at nonstoichiometric values of $x > 0.5$ giving the OI phase. It is obvious that such a location of chains in the OI phase results in the diffraction reflexes of the OII phase. Taking all this into account the interval of the pure OII phase at room temperature in the phase diagram of Fig. 5 ($0.47 < x < 0.54$) has to be extended for comparison with the experimental phase diagrams. Then this interval correlates quite nicely with the OII-phase interval shown in Fig. 1 as well as with the interval $0.48 < x < 0.62$ observed for the samples exhibiting the best OII-phase reflections.[3]

III. CHAIN LENGTH

To obtain the average length of the O-Cu-O chain (or the length of sequentially sited oxygen atoms) in the basal plane, one has to calculate, using the CVM, the two-particle intra-chain correlator $g_k(+,+) = \langle n_i^k n_{i+1}^k \rangle$, which corresponds to the concentration of sequentially occupied pairs of oxygen atoms (the probability that in a pair of neighboring sites both sites are occupied), or the two-particle intrachain correlator $g(+,-) = \langle n_i^k (1 - n_{i+1}^k) \rangle$, characterizing chain ends (the probability that in a pair of neighboring sites one is occupied and another is empty). Here the index k stands for the denotation of sublattice O(1) or O(5) and "$+(-)$" stands for the occupied (empty) site. The calculation of $g_k(+,+)$ by the CVM demonstrates[26] that $g_k(+,+)$ with a decrease in temperature approaches the value of the sublattice concentration $c_k = \langle n_i^k \rangle = g_k(+,+) + g_k(+,-)$, i.e., $g_k(+,-)$ tends to zero. This means that every O-Cu-O chain of sublattices $O(1)_1$ and $O(1)_2$ consists of alternating, considerably long, occupied, and empty segments. The sublattice O(5) is empty of oxygen atoms at low temperatures. The large number of three-coordinated copper (chain ends), and hence the random distribution of vacancies, is less favorable than the arrangement of vacancies and chains in sequential segments as in Fig. 6. When the chain is formed by alternating occupied and empty segments, the concentration of oxygen per chain is equal to $c_k = m_k l_k / N$, where l_k is the average length of the
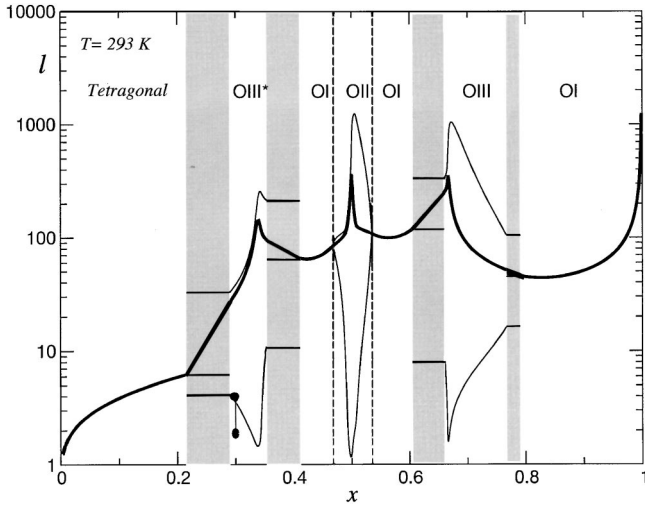
FIG. 7. Average length of O-Cu-O chains as a function of oxygen amount for $0 \leq x \leq 1$. Regions shown in grey denote mixed phases OIII* + OI and OIII + OI. Average length of chain for different sublattices is shown by thin solid lines. Their average [see formula (4)] is shown by the thick solid line. Three thin lines in the region of the mixed phases are obtained for both sublattices of the OIII* or OIII phases (external lines) and the OI phase (middle line). At $x = 0.30$ two experimental points [7] are shown by solid circles.

occupied segment in sublattice k, m_k is the number of segments, and N is the number of sites in a chain. The correlators $g_k(+,+)$ and $g_k(+,-)$ are equal to

$$g_k(+,+) = \frac{m_k(l_k-1)}{N}, \quad g_k(+,-) = \frac{m_k}{N}. \quad (2)$$

As a result, the length of the occupied segment of chain in the kth sublattice is

$$l_k = [1 - g_k(+,+)/c_k]^{-1}. \quad (3)$$

The average length of the chain in the OII and OIII phases is obtained from the formula

$$l_{av} = \frac{am_1 l_1 + m_2 l_2}{am_1 + m_2} = \left[1 - \frac{ag_1(+,+) + g_2(+,+)}{ac_1 + c_2}\right]^{-1}, \quad (4)$$

where $a = 1$ for the OII phase and $a = 2$ for the OIII phase, and the subscripts 1 and 2 are for the sublattices $O(1)_1$ and $O(1)_2$, respectively. The dependence of chain lengths at room temperature and $0 \leq x \leq 1$ as a function of oxygen amount is presented in Fig. 7. The average length of chain l_{av} in all phases of the phase diagram is shown by a thick solid line. This line is obtained for each phase separately using formulas (3) and (4) and connected at the phase boundaries. The maxima of l_{av} are observed at stoichiometric values of each orthorhombic phase ($x = 0.33$, 0.5, 0.67, and 1). The maxima increase drastically with the decrease in temperature, since the more occupied sublattice at $T \to 0$ tends to complete occupation, while the less occupied one tends towards full depletion.[27] Two points at $x = 0.3$, obtained by the NMR experiment[7] for intercalated ($l_{av} = 3.9$) and deintercalated ($l_{av} = 1.9$) samples, are also presented for comparison.

As is seen, our result for the less occupied sublattice in the OIII* phase is consistent with the NMR results, especially for the intercalated sample, though the average length of chain in this phase for chosen values of the interaction constants is somewhat higher and almost equal to that of the more occupied sublattice.

IV. DISCUSSION

The kinetic nature of the experimental phase diagrams should be taken into account when they are compared to calculations based on the thermodynamic equilibrium. In spite of this, an overall good agreement has been found between theory and experiment. The superstructures, characterized by the ordered sequences of full and empty O-Cu-O chains, which were systematically observed by ED in our equilibrated samples, are those expected from the extended ASYNNNI model. Similar superstructures with periodicity exceeding $3a$ have been observed before[5,12] and also recently by neutron- and x-ray-diffraction experiments[2] on single-crystal samples. We also occasionally observed such superstructures in our samples, but, in the absence of systematic experimental evidence, they should be considered for the present more as representing a particular local oxygen arrangement rather than a thermodynamically stable structure. However this point requires a deeper investigation of the dependence of ordering in the critical regions, in particular, on the stabilization temperature and the time of the thermal treatment.

It should also be pointed out that the term OII or OIII region, used in the experimental phase diagram, refers to the existence in the corresponding ED patterns of the superlattice spots $(h/200)$ or $(h/300)$. For the present work all the ED patterns were taken in a selected area mode on a region of about 200 nm in diameter. With the lattice periodicity (of the order of 1 nm) observed in the basal plane of $YBa_2Cu_3O_{6+x}$, structures locally ordered in the range of a few tens of nanometers are sufficient to produce a coherent response to the incident-electron beam. The presence of the diffuse-streaked satellite spots, observed, e.g., for oxygen contents well below the ideal composition of the OII structure $x = 0.5$, is a convincing indication of the tendency of the system to arrange itself locally in ordered domains of a sufficient dimension to produce a detectable diffraction intensity. As discussed above in Sec. II B this picture is not in contradiction with the theoretical expectation that the real thermodynamic phase would be the OI phase, since the absence of long-range correlation among different OII domains results in some ''statistically average'' occupancy of the O-Cu-O chains. The progressive transition observed by increasing x from diffuse-streaked to intense-sharp satellite spots (the latter experimentally observed for the OII and OIII phases at $x = 0.57$ and 0.7, respectively) can be considered as a qualitative confirmation of the progressive extension of the ordering to the entire investigated area.

Since in general the ED patterns do not change significantly within a set of plates coming from the crystallites of the same sample, the short-range ordered domains can be considered as statistically distributed over the whole sample.

A macroscopic phase separation, resulting in a different ED response from different grains of the same sample, was observed only in the transient T-O region. This is probably due to the fact that in the presence of a small amount of carriers the system tends to split into a two-phase state, one poor and the other rich in carriers.

A slight difference between experimental and calculated phase diagrams was found in values of oxygen content x_m, for which the maximum degree of OII and OIII ordering was observed. The values of x_m obtained by ED (0.57 for the OII and 0.7 for the OIII phase) exceed the calculated ones (0.5 and 0.67, respectively) that are imposed by the symmetry of the ASYNNNI model. A possible reason may lie in the influence of ordering kinetics that makes every order-disorder transition a continuous process. By taking into account that the samples were stabilized at $T_s = 75 - 130\,°C$ in a proximity to their transitions OII→OI and OIII→OI and examined at room temperature not so far from T_s, they should possess a certain degree of disorder even for the ideal stoichiometry.

Therefore some excess oxygen could be required to extend the superstructure homogeneously to the whole area investigated by the ED.

V. SUMMARY

A combined experimental and theoretical study of the phase diagram of $YBa_2Cu_3O_{6+x}$ that includes orthorhombic low-temperature superstructures was performed. For the first time the phase diagrams were extended to $x < 0.5$ to include the anti-OIII (OIII*) phase and the transient tetragonal-to-orthorhombic region of the superconductivity onset. The influence of the preparation kinetics on structural and superconducting properties of oxygen-chain-equalized and order-stabilized $YBa_2Cu_3O_{6+x}$ pair samples was discussed for a wide range of oxygen contents. The lengths of O-Cu-O chains were calculated for different orthorhombic phases and compared, where possible, with NQR results previously reported.

*Deceased.

[1] G. Calestani, P. Manca, S. Sanna, and A. Migliori, Int. J. Mod. Phys. A **13**, 1073 (1999).

[2] N.H. Andersen, M. von Zimmermann, T. Frello, M. Käll, D. Mønster, P.-A. Lindgård, J. Madsen, T. Niemöller, H.F. Poulsen, O. Schmidt, J.R. Schneider, Th. Wolf, P. Dosanjh, R. Liang, and W.N. Hardy, Physica C **317-318**, 259 (1999).

[3] F. Yakhou, J.-Y. Henry, P. Burlet, V.P. Plakhty, M. Vlasov, and S. Moshkin, Physica C **333**, 146 (2000).

[4] D.J. Werder, C.H. Chen, R.J. Cava, and B. Batlogg, Phys. Rev. B **37**, 2317 (1988); **38**, 5130 (1988).

[5] R. Beyers, B.T. Ahn, G. Gorman, V.Y. Lee, S.S. Parkin, M.L. Ramires, K.P. Roche, J.E. Vazquez, T.M. Gür, and R.A. Huggins, Nature (London) **340**, 619 (1989).

[6] P. Manca, P. Sirigu, G. Calestani, and A. Migliori, Nuovo Cimento Soc. Ital. Fis., D **19D**, 1009 (1997).

[7] P. Manca, S. Sanna, G. Calestani, A. Migliori, R. De Renzi, and G. Allodi, Phys. Rev. B **61**, 15 450 (2000).

[8] T. Zeiske, D. Hohlwein, R. Sonntag, F. Kubanek, and T. Wolf, Physica C **194**, 1 (1992); D. Hohlwein, in *Materials and Crystallographic Aspects of High-T$_c$ Superconductivity*, edited by E. Kaldis (Kluwer Press, Dordrecht, 1994).

[9] P. Schleger, H. Casalta, R. Hadfield, H.F. Poulsen, M. von Zimmermann, N.H. Andersen, J.R. Schneider, Ruixing Liang, P. Dosanjh, and W.N. Hardy, Physica C **241**, 103 (1995).

[10] P. Schleger, R. Hadfield, H. Casalta, N.H. Andersen, H.F. Poulsen, M. von Zimmermann, J.R. Schneider, Ruixing Liang, P. Dosanjh, and W.N. Hardy, Phys. Rev. Lett. **74**, 1446 (1995).

[11] V. Plakhty, A. Stratilatov, Yu. Chernenkov, V. Fedorov, S.K. Sinha, C.K. Loong, B. Gaulin, M. Vlasov, and S. Moshkin, Solid State Commun. **84**, 635 (1992); A. Stratilatov, V. Plakhty,

Yu. Chernenkov, and V. Fedorov, Phys. Lett. A **180**, 137 (1993).

[12] J. Reyes-Gasga, T. Krekels, G. van Tendeloo, J. van Landuyt, S. Amenlinckx, W.H.M. Bruggink, and M. Verwej, Physica C **159**, 831 (1989).

[13] S. Yang, H. Claus, B.W. Veal, R. Wheeler, A.P. Paulikas, and J.W. Downey, Physica C **193**, 243 (1992).

[14] L.T. Wille, A. Berrera, and D. de Fontaine, Phys. Rev. Lett. **60**, 1065 (1988).

[15] V.E. Zubkus, S. Lapinskas, and E.E. Tornau, Physica C **166**, 472 (1990).

[16] D. de Fontaine, G. Ceder, and M. Asta, Nature (London) **343**, 544 (1990).

[17] S. Lapinskas, E.E. Tornau, A. Rosengren, and P. Schleger, Phys. Rev. B **52**, 15 565 (1995).

[18] G. Ceder, M. Asta, and D. de Fontaine, Physica C **177**, 106 (1991).

[19] V.E. Zubkus, S. Lapinskas, A. Rosengren, and E.E. Tornau, Physica C **206**, 155 (1993).

[20] G.V. Uimin, V.F. Gantmakher, A.M. Neminsky, L.A. Novomlinky, D.V. Shovkun, and P. Brüll, Physica C **192**, 481 (1992).

[21] S. Semenovskaya and A.G. Khachaturyan, Phys. Rev. B **51**, 8409 (1995); **54**, 7545 (1996).

[22] A.A. Aligia, Europhys. Lett. **18**, 181 (1992).

[23] M. Muroi and R. Street, Physica C **246**, 357 (1995).

[24] P.E. Sterne and L.T. Wille, Physica C **162-164**, 223 (1989).

[25] D.J. Liu, T.L. Einstein, P.A. Sterne, and L.T. Wille, Phys. Rev. B **52**, 9784 (1995).

[26] V.E. Zubkus, S. Lapinskas, and E.E. Tornau, Physica C **159**, 501 (1989).

[27] E.E. Tornau, S. Lapinskas, A. Rosengren, and V.M. Matic, Phys. Rev. B **49**, 15 952 (1994).